ARCHIVES OF METALLURGY AND MATERIALS
Volume 53 2008 Issue 3

G. ZHU*, **, X. P. ZOU*, J. CHENG*, M. F. WANG*, Y. SU*

SYNTHESIS AND CHARACTERIZATION OF SiO_2 AND SiC MICRO/NANOSTRUCTURES

SYNTEZA I CHARAKTERYSTYKA MIKRO/NANOSTRUKTUR SiO_2 I SiC

Silica-based nanowires, straight nanorods, straight Y-shaped silica nanorods, flower-like microstructures, and SiC/SiO_2 core-shell coaxial nanocables have been generated through a simple thermal evaporation method. The synthesized samples were characterized by means of scanning electron microscopy, transmission electron microscopy, high resolution transmission electron microscopy, energy dispersive X-ray spectroscopy, and Raman spectrum. Generated silica nanowires with a diameter of about 100nm and length of up to several tens of micrometers, straight silica nanorods and Y-shaped nanorods with a diameter about 50-200nm, and novel flower-like silica microstructures all are amorphous and consist only of silicon oxide, and have a neat smooth surface. Generated SiC/SiO_2 core-shell coaxial nanocables have a crystalline core and a surrounding amorphous layer. The results show that the present method should be possible to synthesis various micro/nanostructures under appropriate experimental conditions. These nanostructures may find applications as building blocks in nanomechanical or nanoelectronic devices.

Keywords: silica; silicon carbide; nanowires; nanorods; flower-like microstructures; coaxial nanocables

Nanodruty na podłożu SiO_2, proste (straight) nanopręty, krzemionkowe nanopręty w kształcie litery Y, mikrostruktury kwiatowe, SiC/SiO2 rdzeniowo-powłokowe kable koncentryczne zostały wytworzone przy zastosowaniu prostej metody odparowania cieplnego. Poddane syntezie próbki scharakteryzowano przy pomocy skaningowej mikroskopii elektronowej, transmisyjnej mikroskopii elektonowej, wysoko rozdzielczej transmisyjnej mikroskopii elektronowej, rentgenospektroskopii z dyspresją energii widma oraz widmaRaman'a. Wytworzone krzemionkowe mikrodruty o średnicy około 100nm oraz długości dochodzącej do kilkudziesięciu mikrometyrów, proste (straight) krzeminokowe nanoprety oraz nanopręty w kształcie litery Y o średnicy około 50-200nm jak również krzemionkowe mikrostruktury kwiatowe są wszystkie amorficzne i składaja się jedynie z tlenku krzemowego wykazując uporządkowaną, gładką powierzchnię. Wytworzone SiC/SiO_2 rdzeniowo-powłokowe kable koncentryczne posiadają rdzeń krystaliczny oraz otaczają go warstwa amorficzną. Wyniki wykazują, że metoda o której mowa może być zastosowana do syntezy różnych mikro/nanostruktur przy zachowaniu odpowiednich reżimów eksperymentalnych. Nanostruktury, o których mowa, mogą znaleźć zastosowanie jako bloki konstrukcyjne w urządzeniach mechanicznych i nanoelektrycznych.

1. Introduction

Since silica nanotubes have been first reported by Nakamura in 1995 [1], there has been an increasing interest to the synthesis of various quasi one-dimensional nanosized materials such as nanotubes, nanowires, nanorods etc.. These one-dimensional nanomaterials show some novel physical and chemical properties due to their peculiar structure and size effect, and they are one of the most promising elements for the fabrication of nanoelectronic devices [2, 3] and integrated optical device [4]. Among them, as an important member in the one-dimensional nanomaterials family, silica-based nanomaterials have been actively studied for a long time. Silica-based nanomaterials with various microstructures have been synthesized utilizing a variety of methods, such as, laser ablation [5, 6], chemical vapor deposition (CVD) [7], discharge [8], vapor-liquid-solid (VLS) [9], vapor-solid (VS) [10], and sol-gel [11] methods. Most previous methods required a vacuum environment and metal catalysis to grow silica-based nanomaterials. We have synthesized silica-based micro/nanostructures using a simple direct thermal evaporation method in ambient

* BEIJING INFORMATION SCIENCE & TECHNOLOGY UNIVERSITY, BEIJING KEY LABORATORY FOR SENSOR, JIANXIANGQIAO CAMPUS, BEIJING 100101, CHINA
** SUZHOU COLLEGE, ANHUI 234000, CHINA

atmosphere. The products were directly deposited on the substrate.

In this paper, we report the direct synthesis of large-scale various silica-based micro/nanostructures by using a sample thermal evaporation method. Compared with the reported synthetic methods for various silica-based micro/nanostructures, the fabrication technique used in this work possesses the virtues including simplicity, low cost, absence of catalyst and template.

2. Experimental procedures

Silica-based nanowires, straight nanorods, straight Y-shaped silica nanorods, flower-like microstructures, and SiC/SiO_2 core-shell coaxial nanocables were prepared in a horizontal electronic resistance tube furnace with a gas supply and a control system. Fig. 1 shows a schematic diagram of the experimental setup employed during the course of the present work. A p-type Si (111) plate ($9\times2.5\times0.05$ cm^3) or quartz ($9\times2.5\times0.1$ cm^3) plate was used as substrate for the growth of the silica-based nanostructures. The plate was ultrasonically washed in acetone for several minutes to clean the surface of wafer, and then rinsed with deionized water. Then appropriately chosen mixtures at a proper weight ratio was placed in a ceramic boat that covered with cleaned substrate, and then the boat was transferred into the centre of a ceramic tube mounted in the horizontal tube furnace with diameter 4.5 cm.

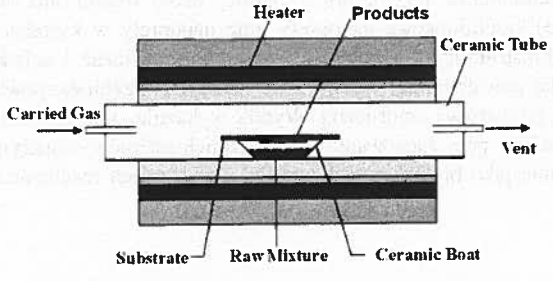

Fig. 1. A schematic diagram of the experimental setup

To prepare the silica nanowires, straight silica nanorods, straight Y-shaped silica nanorods, and flower-like silica microstructures, a SiO_2/carbon nanofibers (Here, silica powder and carbon nanofibers are synthesized by combustion and CVD method in our laboratory, respectively) or Si(99.00%, Shanghai Chemical Co.)/SiO(99.00%, Beijing Chemical Reagents Co.)/active cabon(Analytically pure, Beijing Chemical Reagents Co.) mixture as starting materials is used at typical central region operating temperatures. The coaxial SiC/SiO_2 core-shell coaxial nanocables are prepared using SiO/active carbon mixture as starting materials. Fig.1

As the starting material mixture vaporizes, the tube furnace was purged with N_2 gas for 30 min to eliminate air in the furnace. Under the ambient pressure and a constant flow of the mixture gas 3% H_2/Ar and N_2 were introduced into the tube, the furnace temperature was heated to desired temperature and held for 2 h. Then the furnace was cooled naturally to room temperature with protection gas. The products were collected on the surface of substrates, respectively.

The parameters controlled in these experiments, in addition to starting material composition are:

1. The entrainment gas flow rate which can range from 100 to 200 sccm.
2. The tube furnace central region temperature.
3. The decline ratio of temperature during tube furnace cooling.

The tube furnace system, including ceramic boat and insulation, is carefully cleaned with deionized water before each set of experiments. With a careful balance of the parameters we have outlined, it is possible to evaluate the "sweet zones" for a number of nanostructure syntheses. As we consider their individual usage, we will outline the specific experimental conditions for each micro/nanostructure synthesis.

The morphology of silica-based micro/nanostructures was examined by scanning electron microscopy (SEM, JEOL 6500F). Further detailed structural information of the products was obtained by transmission electron microscope (TEM) (JEOL-2010), selected-area electron diffraction (SAED). The chemical composition of the materials under study was determined by energy dispersive X-ray spectroscopy (EDS).The specimens for TEM analysis were prepared by dispersing the samples in ethanol followed by sonication for 10 min. A few drops of the suspension were dropped onto a copper microgrid covered with a holey carbon thin film. The structure of the resulting products was characterized by using a M21XVHF2Z (Mac Science Co. Ltd) X-ray diffractometer with Cu Kα radiation at room temperature. The Raman spectrum was measured with a Rainshaw optical confocal Raman spectrometer at room temperature. The 514 nm line of an Ar^+ laser was used as the excitation source.

3. Synthesis and characterization of SiO_2 and SiC micro/nanostructures

3.1. Silica nanowires

Silica nanowires have been synthesized by thermal evaporation of mixed powders of silica and carbon nanofibers and condensation on quartz substrate. The raw material was a mixture of silica and carbon

nanofibers powders at a weight ratio of 2:1. The furnace temperature was heated to 1200° and held for 2 h under the ambient pressure and a constant flow of the mixture gas 3% H_2/Ar (50sccm) and N_2 (50sccm) were introduced into the tube. After furnace was cooled down to about 700° at 10°/min, and then cooled naturally to room temperature with carried gas.

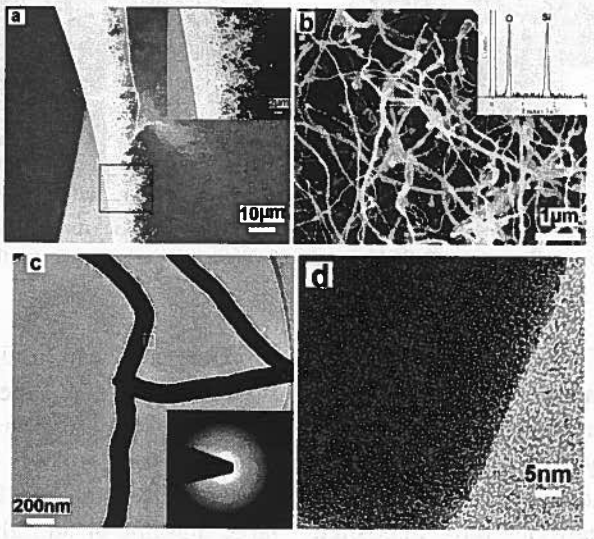

Fig. 2. (a) Side view SEM image of silica nanowires; (b) Up-down SEM image of silica nanowires and the inset is corresponding EDS; (c) TEM image of silica nanowires and the inset is corresponding SAED; (d) HRTEM image of (c)

Fig.2 is the SEM and TEM images of silica nanowires obtained on quartz substrate. The side view image of silica nanowires (Fig. 2a) shows that silica nanowires are curved. The inset of Fig.2a is the close view image of the black pane area marked in Fig.2a. The Fig.2b is a up-down SEM image of silica nanowires, which indicates that silica nanowires have lengths of about 10μm and diameters of about 100nm. The EDS (attached to the SEM) spectrum in the inset of Fig.2b displays that nanowires are composed of Si and O. Low magnification transmission electron microscopy (Fig. 2c) shows these the silica nanowires have a diameter of about 100nm neat smooth surface. The corresponding selected area diffraction pattern (inset in Fig.2c) with only diffusive rings (without diffraction spots) reveals the amorphous nature of the silica nanowires. Fig. 2d is the HRTEM image of the white rectangular area marked in Fig. 2c, revealing that no fringes exist in the silica nanowires.

3.2. Straight silica nanorods and straight Y-shaped silica nanorods

The straight silica nanorods and straight Y-shaped silica nanorods have been synthesized by thermal evaporation method and condensation on Si substrate. We used 1300° instead of 1200° as synthesis temperature in the experimental process, with the other experimental parameters being identical, respectively.

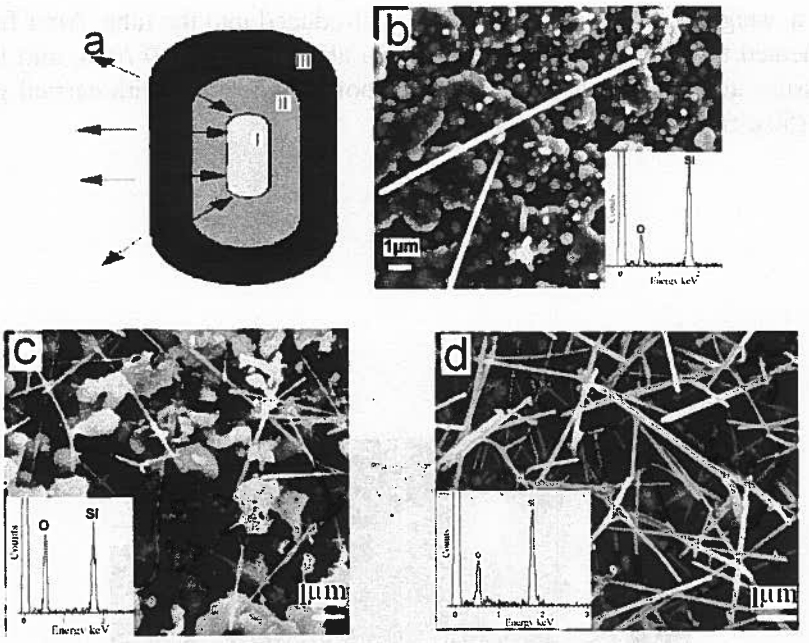

Fig. 3. (a) Schematic diagram depicting different growth zones; (b) SEM image of silica nanorods grown on the zone I in (a); (c) SEM image of silica nanorods grown on the zone II in (a); (d) SEM image of silica nanorods grown on the zone III in (a)

Fig.3 is the SEM images of silica nanorods grown on Si substrate. However, it is amazed at the different morphology of silica nanorods are found on the Si substrate. Fig.3a shows schematically different growth zones of the silica nanorods on the Si substrate. From Fig.3b, it clearly shows some silica nanoparticles have deposited on the zone I (Fig.3a light zone) and some nuclei of silica nanorods have also formed. Fig.3c shows a few of silica nanorodsare synthesized on the zone II (Fig. 3a grey zones), and Fig.3d shows a large amount of silica nanorods are synthesized on the zone III (Fig.3a black zone). The EDS spectrums (insets of Fig.3b, c and d) all show the products grown on different zones consisting of elements Si and O with an atomic ratio about 1:2. Well then what leads to the formation of the phenomenon here?

Although the detailed mechanism for the formation of different morphologies of silica nanorods structures is not well understood, we still believe that the different local concentrations of the SiO_2 may be responsible for the different morphologies of rods structures. A possible explanation is depicted as follows: when the furnace is heated to high temperature, the growth temperature is high enough to produce vapor SiO_2 in the ceramic boat. As the process proceeds, a continuous accumulation of the vapor SiO_2 in the ceramic boat leads to a continuous increase of vapor pressure and vapor concentration of SiO_2. However, their concentrations would increase gradually with the increasing distance from the centre position of growth substrate. These vapors SiO_2 will diffuse along in all directions at the growth zone III (black arrows in Fig. 3a), where is the joint between substrate and boat. So the concentration gradient of SiO_2 is formed and distributed along the radial in the ceramic boat. At the deposition area near the Zone III, the concentration of the SiO_2 is relatively high, and the silica nanorods would grow fast and long. The presence of a large amount of straight nanorods should be attributed to the strong limiting effect of the high SiO_2 concentration to the silica nanostructures surface (see Fig.3d). If the SiO_2 concentration was reduced a little (zone II), a small quantity of silica nanorods are synthesized on the growth substrate. In the mean time, the second nucleation perhaps could not achieve and finally only leaving the straight silica nanorods (see Fig.3c). If the SiO_2 concentration reduced more (zone I), few silica nanorods are achieved and only leaving the nuclei of silica nanorods (see Fig.3b).

The straight Y-shaped silica nanorods have also been found on the growth zone III of Si substrate (Fig.3a black zone). It can be clearly seen that the as-synthesized products consists of many Y-shaped silica nanorods with straight branches (Fig. 4a). Some silicon oxide nanorods branched several times to form multiple Y junctions, which still keep their branches straight. Fig. 4b is the close view image of the white pane area marked in Fig.4a, which shows that a straight Y-shaped silica nanorods with neat smooth surface and uniform branches of about 180 nm in diameter. The angles between the three branches in sample have been measured on 10 different Y-shaped silica nanorods from SEM images. As a result, the angles are close to 120°. All the Y junctions have very similar shape regardless of their different diameters.

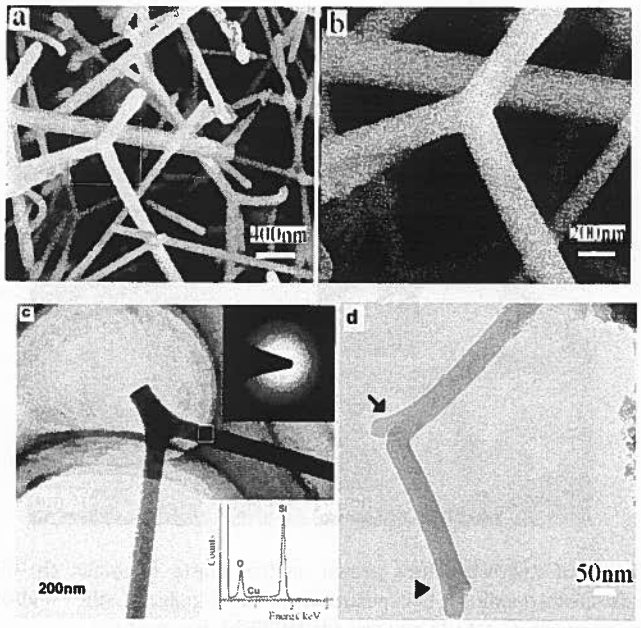

Fig. 4. (a) SEM image of straight Y-shaped silica nanorods; (b) Closer view showing Y-shape nanostructures in (a); (c) TEM images of straight Y-shaped silica nanorods, the top right inset is the corresponding EDS spectrum, and the bottom right inset is corresponding SAED pattern; (d) A double Y-shape nanostructures

Fig.4c is typical TEM image of a straight Y-shaped silica nanorod, which indicates that rod has neat smooth surfaces with diameter of about 100nm. The top right inset of Fig.4c is the corresponding EDS spectrum displays that Y-shaped silica nanorods consisting of elements Si and O with an atomic ratio about 1:2. The Cu peaks come from the TEM grid. The bottom right inset of Fig.4c is selected-area electron diffraction (SAED) pattern from white pane area marked in one branches with only diffusive rings (without diffraction spots), revealing the amorphous nature of the silicon oxide nanorods. Figure 4d shows a double straight Y junction with short and long branches. All branches have the same diameters in the double Y-shaped structures, in agreement with SEM observations.

For the formation of straight Y-shaped silica nanorods, the detailed description as follows: At the deposition area near the Zone III, the concentration of the SiO_2 is the highest above the Si substrate, which results in the formation of a large amount of straight silica nanorods. At the same time, the high concentration silicon oxide would provide a second nucleation on the side surface (indicated by arrow in Fig.4d) or top (indicated by arrowhead in Fig.4d) of a developed rod. As a result, the growth process of silicon oxide nanorods could be altered, forming the split of the surface of rod. At last, the straight Y-shaped silica nanorods would be formed by depositing silicon oxide continuously.

3.3. Flower-like silica microstructures

Flower-like silica microstructures have been synthesized by thermal evaporation at 1050° and condensation on quartz substrate. The raw material was a mixture of Si/SiO/active carbon powders at a weight ratio of 6:3:4, with the other experimental parameters being identical, respectively.

A low-magnification SEM image (Fig. 5a) shows that the flower-like silica microstructures grown on the quartz substrate, which shows that the flower-like microstructures are made up of many microwires. All the microwires have cone-shaped tips at their ends. In addition, these wires are rooted in one center and have a length of several micrometers, and the diameter of microwires decrease along with the growth of microwires increase. Fig. 5b is the closer view image in Fig. 5a, which shows that the surface of nanowires is neat and smooth. The EDS (inset in Fig. 5B) indicates these wires consist of elements Si and O with an atomic ratio about 1:2.

The morphology and structure of flower-like silica microstructures have been characterized in further detail using TEM and selected area electron diffraction (SAED). Some short wires with length of about several μm are shown in Fig. 5c. They may be broken from a whole flower-like silica microstructure because of the ultrasonic vibrations. The inset of Fig. 5c is selected-area electron diffraction (SAED) pattern from white rotundity area marked in Fig. 5c with only diffusive rings (without diffraction spots), revealing the amorphous nature of the silica microwires. Fig. 5d is the HRTEM image of the white pane area marked in Fig. 5c, revealing that no fringes exist in the silica microwires.

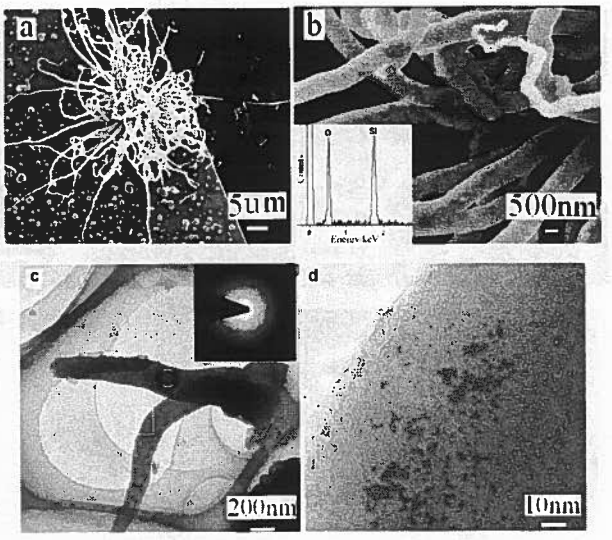

Fig. 5. (a) SEM image of flower-like silica microstructures grown on the quartz substrate; (b) Closer view showing flower-like silica microstructures in (a) and the inset is the corresponding EDS spectrum; (c) TEM image of silica microstructures (broken from the flower-like microstructures) and the inset is the corresponding SAED pattern; (d) HRTEM image of (c)

For the formation of flower-like silica microstructures, it could be considered that it via both of VS process and the OAG [12] process. In the initial stage, a large amount of silica particles have deposited on the surface of the substrate and some nuclei of silica microwires have also formed, which is described as the VS process. Then, the newly formed silica will stack on the silicon oxide nuclei, forming silica microwires on the substrate, which is described as the OAG process. In the mean time, a lot of silica wires grow and aggregate in one center. As a result, flower-like microstructures are formed. At last, the novel flower-like silica microstructures would be formed by growing continuously silica microwires in one centre.

3.4. SiC/SiO_2 core-shell coaxial nanocables

SiC/SiO_2 core-shell coaxial nanocables have been synthesized through thermal evaporation method and condensation on Si substrate without assistance of any catalyst. The raw material was a mixture of SiO and active carbon at a weight ratio of 1:2. The furnace temperature was heated to 1300°C and held for 2 h under the ambient pressure and a constant flow of the mixture gas 3% H_2/Ar (100 sccm) and N_2 (100 sccm) were introduced into the tube, with the other experimental parameters being identical, respectively.

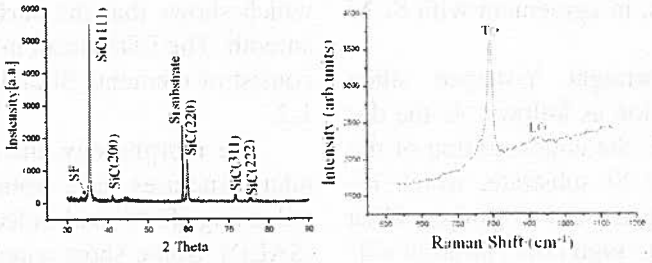

Fig. 6. (a) Side view SEM image of silica nanowires; (b) Up-down SEM image of silica nanowires and the inset is corresponding EDS; (c) TEM image of silica nanowires and the inset is corresponding SAED; (d) HRTEM image of (c)

The products grown on the Si substrate were checked using XRD and the result is shown in Fig. 6a. The main strong diffraction peaks can be indexed to the zinc-blende structure, which indicates the crystalline SiC core have a β-SiC structure (JCPSD file: 29-1129). A small peak marked SF, corresponding to stacking faults, is also shown in the spectrum [13]. The stronger intensities of β-SiC diffraction peaks (relative to the background amorphous) indicate that the resulting products were well-crystallized β-SiC. In addition, XRD pattern

of the synthesized SiC/SiO_2 nanocables also shows no difference except broad diffraction peak compared to SiC nanowires, which maybe the result of the effect of nanosize and surface states. Si diffraction peaks in the pattern come from the Si substrate.

Raman spectra of the SiC/SiO_2 core-shell coaxial nanocables (Fig. 6b) were obtained at room temperature with an excitation wavelength of 514 nm (Ar^+ ion laser). Two peaks (around 794 and 947 cm^{-1}) are observed. These correspond to the transverse optical (TO) mode and longitudinal optical (LO) mode phonons of cubic SiC, and confirm the presence of crystalline β-SiC nanostructures [14]. Both peaks have redshifts with respect to the TO and LO photomodes of bulk β-SiC, respectively, which could either be ascribed to quantum confinement effects or the stacking faults and inner stress during the growth [15].

Low magnification TEM image (Fig.7a) shows that there were straight wire-like structures, all with uniform diameters. The EDS spectrum in the inset displays that the nanowires are composed of Si, C and O. The Cu peaks come from the TEM grid. With increasing magnification (the black pane area marked in Fig. 7a), we observe that the nanowires are in fact of a clear coaxial core-shell cable nanostructure (as shown in Fig. 7b). These nanocables have a crystalline core and a surrounding amorphous layer. The outer amorphous SiO_2 sheath usually has a uniform thickness, dependent of the core diameter. And according the observation of TEM images, we speculate that the thickness of outer amorphous SiO_2 sheath is in direct ration to the diameter of core. It also indicates step-like streaked lines, which suggest that the SiC core possess a high density of planar defects and stacking faults. We believe that these planar defects occur during the growth process due to thermal stress [16]. The corresponding selected area diffraction pattern (Fig. 7c) from black rotundity area marked in Fig. 7b indicates that the crystalline core is β-phase SiC, with the $< 110 >$ axis parallel to the electron beam. Diffraction spots from {111} planes were labeled, with T representing twinning planes. Form the HRTEM image (Fig. 7d) from the black rectangular area marked in Fig. 7b, we can see the typical $< 110 >$ projection of a face-centered cubic structure with (111) plane spacing of about 0.25 nm, suggesting that the axes of the SiC core lie along the [111] direction. The structure shown here is similar to that of a coaxial cable conventionally used in signal transmission, so we call it a coaxial nanocable [17].

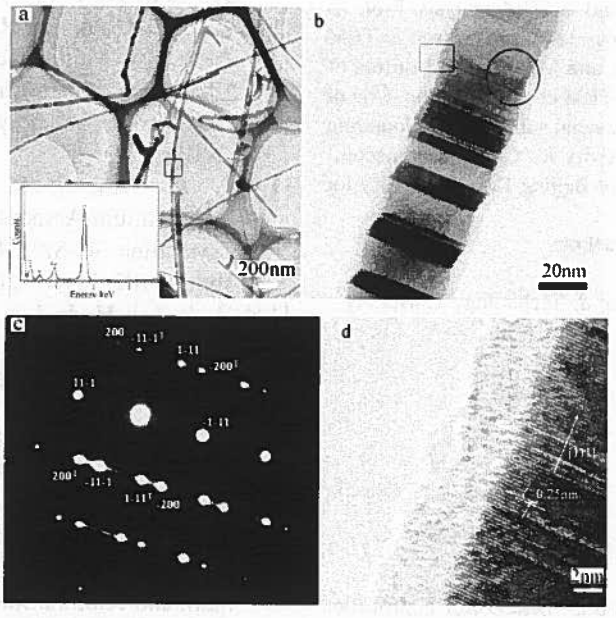

Fig. 7. (a) TEM image of SiC/SiO_2 core-shell coaxial nanocables and the inset is EDS spectrum of individual nanocable. (b) Magnified image in (a) shows a crystalline core and an amorphous layer. (c) The corresponding SAED pattern taken from black rotundity area marked in (b). (d) High-resolution image of the nanocable taken from the black rectangular area marked in (b)

The formation of SiC/SiO_2 core-shell coaxial nanocables through a reaction [17]:

C (solid or vapor) + SiO (gas) → SiC (solid) + SiO_2 (solid)

the whole growth process may be dominated by a double vapor-solid process. The first VS step is the growth of crystalline SiC core, this procedure occurs during the calefactive and holding stage. The second VS step is the deposition of SiC and SiO_2 on the surface of the as-grown SiC core; this procedure takes place in the

cooling stage at temperatures below 900°. SiO_2 and SiC deposit onto the surface of the grown-up SiC core, by reason of the difference of density and the good fluidity of SiO_2 at this temperature, these two materials can be separated easily during growth and thus form SiC/SiO_2 core-shell coaxial nanocables in the end.

4. Conclusion

Silica-based nanowires, straight nanorods, straight Y-shaped silica nanorods, flower-like microstructures, and SiC/SiO_2 core-shell coaxial nanocables have been synthesized through using simple thermal evaporation method. Investigation results that the formation of silica nanowires, straight nanorods, and straight Y-shaped silica nanorods all are via a simple VS process, flower-like silica microstructures is via both of VS process and the OAG process, and SiC/SiO_2 core-shell coaxial nanocables is via a double vapor-solid process. Such silica-based micro/nanostructures may have wide ranges of applications in nanoelectronics, nanomechanics, reinforced composite materials, or nanosensors.

Acknowledgements

The authors thank Prof. X. M. Meng of Technical Institute of Physics and Chemistry of CAS for the aid in SEM analysis, Prof. X. D. Xu of Beijing University of Technology for the assistance in TEM analysis, and Prof. W. Xu, Mr. Su, Sun, and Miss Sun of Institute of Biophysics of CAS for the assistance in TEM characterization. One of Authors (X.P. Zou) thanks the partial financial support from Founding Program of Science & Technology Activity for Chinese Homecoming Fellow Abroad, Research Program of Beijing Key Laboratory for Sensor (No.KM200810772009).

Address of the corresponding author:
Author: Prof. Xiaoping Zou
Institute: Beijing Information Science & Technology University
City: Beijing.
Country: China
Telephone: +86-10-64884673-816
Fax: +86-10-64879486
Email: xpzou2005@gmail.com

REFERENCES

[1] H. Nakamura, Y. Matsui, "Silica Gel Nanotubes Obtained by the Sol-Gel Method", J. Am. Chem. Soc. **117**, 2651-2653 (1995).

[2] H. Dai, E. W. Wong, Lieber C.M., "Probing Electrical Transport in Nanomaterials: Conductivity of Individual Carbon Nanotubes", Science **272**, 523-526 (1996).

[3] T. W. Ebbesen, H. J. Lezec, H. Hiura, J. W. Bennett, "Electrical conductivity of individual carbon nanotubes", Nature **382**, 54-56 (1996).

[4] D. P. Yu, Q. L. Hang, Y. Ding, "Amorphous silica nanowires: Intensive blue light emitters", Appl. Phys. Lett. **73**, 3076-3079 (1998).

[5] A. M. Morales, C. M. Lieber, "A Laser Ablation Method for the Synthesis of Crystalline Semiconductor Nanowires", Science **279**, 208-211 1998.

[6] W. Shi, H. Zheng, H. Peng, N. Wang, C. S. Lee, S. T. Lee, "Laser Ablation Synthesis and Optical Characterization of Silicon Carbide Nanowires", J. Am. Chem. Soc, **83**, 3228-3230 (2000).

[7] H. F. Zhang, C. M. Wang, S. L. Wang, "Helical Crystalline SiC/SiO_2 Core-Shell Nanowires", Nano Lett. **2**, 941-944 (2002).

[8] T. Seeger, P. K. Redlich, M. Rühle, "Synthesis of Nanometer-Sized SiC Whiskers in the Arc-Discharge", Adv. Mater. **12**, 279-282 (2000).

[9] C. H. Liang, L. D. Zhang, G. W. Meng, "Preparation and characterization of amorphous SiOx nanowires", J. Non-Cryst. Solids **277**, 63-67 (2000).

[10] X. S. Peng, X. F. Wang, J. Zhang, "Synthesis and characterization of ultra-long silica nanowires", Appl. Phys. A **74**, 831-835 (2002).

[11] M. Zhang, Y. Bando, L. Wada, "Synthesis of Nanotubes and Nanowires of Silicon Oxide", J. Mater. Sci. Lett. **18**, 1911-1914 (1999).

[12] Z. W. Pan, Z. R. Dai, L. Xu, S. T. Lee, Z. L. Wang, "Temperature-Controlled Growth of Silicon-Based Nanostructures by Thermal Evaporation of SiO Powders", J. Phys. Chem. B, Vol. **105**, 2507-2514 (2001).

[13] G. C. Xi, Y. Y. Peng, S. G. Wan, T. W. Li, "Lithium-Assisted Synthesis and Characterization of Crystalline 3C-SiC Nanobelts", J. Phys. Chem. B, Vol. **108**, 20102-20104 (2004).

[14] Z. J. Li, H. J. Li, X. L. Chen, A. L. Meng, K. Z. Li, X. P. Xu, L. Dai, "Large-scale synthesis of crystalline β-SiC nanowires", Appl. Phys. A **76**, 637-640 (2003).

[15] S. Nakashima, H. Harima, "Raman Investigation of SiC Polytypes", Physica Status Solidi (A), Applied Research **162**, 39-64 (1997).

[16] Z. J. Li, J. I. Zhang, A. Meng, "Large-Area Highly-Oriented SiC Nanowire Arrays: Synthesis, Raman, and Photoluminescence Properties", J. Phys. Chem. B **110**, 22382-22386 (2006).

[17] Y. Zhang, K. Suenaga, C. Colliex, S. Iijima, "Coaxial Nanocable: Silicon Carbide and Silicon Oxide Sheathed with Boron Nitride and Carbon", Science **281**, 973-975 (1998).

Received: 12 February 2008.